Biochem. J. (2013) **449**, 151–159 (Printed in Great Britain) doi:10.1042/BJ20121280

Small-molecule inhibition of MLL activity by disruption of its interaction with WDR5

Guillermo SENISTERRA*[1], Hong WU*[1], Abdellah ALLALI-HASSANI*[1], Gregory A. WASNEY*[1], Dalia BARSYTE-LOVEJOY*, Ludmila DOMBROVSKI*, Aiping DONG*, Kong T. NGUYEN*, David SMIL*, Yuri BOLSHAN*, Taraneh HAJIAN*, Hao HE*, Alma SEITOVA*, Irene CHAU*, Fengling LI*, Gennadiy PODA†, Jean-François COUTURE‡, Peter J. BROWN*, Rima AL-AWAR†, Matthieu SCHAPIRA*§, Cheryl H. ARROWSMITH*‖[2] and Masoud VEDADI*[2]

*Structural Genomics Consortium, 101 College Street, Toronto, Ontario, Canada, M5G 1L7, †Medicinal Chemistry Platform, Ontario Institute for Cancer Research, MaRS Centre, South Tower, 101 College Street, Toronto, Ontario, Canada, M5G 0A3, ‡Ottawa Institute of Systems Biology, Department of Biochemistry, Microbiology and Immunology, University of Ottawa, 451 Smyth Road, Ottawa, Ontario, Canada, K1H 8M5, §Department of Pharmacology and Toxicology, University of Toronto, 1 King's College Circle, Toronto, Ontario, Canada, M5S 1A8, and ‖Ontario Cancer Institute, The Campbell Family Institute for Cancer Research and Department of Medical Biophysics, University of Toronto, 1 King's College Circle, Toronto, Ontario, Canada, M5S 1A8

WDR5 (WD40 repeat protein 5) is an essential component of the human trithorax-like family of SET1 [Su(var)3–9 enhancer-of-zeste trithorax 1] methyltransferase complexes that carry out trimethylation of histone 3 Lys[4] (H3K4me3), play key roles in development and are abnormally expressed in many cancers. In the present study, we show that the interaction between WDR5 and peptides from the catalytic domain of MLL (mixed-lineage leukaemia protein) (KMT2) can be antagonized with a small molecule. Structural and biophysical analysis show that this antagonist binds in the WDR5 peptide-binding pocket with a K_d of 450 nM and inhibits the catalytic activity of the MLL core complex *in vitro*. The degree of inhibition was enhanced at lower protein concentrations consistent with a role for WDR5 in directly stabilizing the MLL multiprotein complex. Our data demonstrate inhibition of an important protein–protein interaction and form the basis for further development of inhibitors of WDR5-dependent enzymes implicated in MLL-rearranged leukaemias or other cancers.

Key words: histone methyltransferase, leukaemia, mixed-lineage leukemia protein (MLL), WD40 repeat protein 5 (WDR5).

INTRODUCTION

Post-translational modifications of histones serve as signals that help govern the transition between transcriptionally active and transcriptionally silent chromatin states [1,2]. For example, trimethylation of Lys[4] of histone H3 (H3K4me3) is associated with active promoters of gene transcription. In mammals, H3K4 is methylated by several HMTs (histone methyltransferases) including the trithorax-related SET1 [Su(var)3–9 enhancer-of-zeste trithorax 1] family of HMTs, which comprise SET1a, SET1b and MLL (mixed-lineage leukaemia protein) 1–4. These enzymes are components of conserved macromolecular complexes that require the effector protein WDR5 (WD40 repeat protein 5) for assembly and activity [3]. The most well characterized of the SET1 proteins is MLL1 (hereinafter referred to as MLL), a key developmental protein that sustains the expression of selected target Hox genes required for proper embryonic development including the haemopoietic system [4], myogenesis [5] and neurogenesis [6].

The *MLL* gene is frequently rearranged in acute myeloid and lymphoblastic leukaemias in adults and children; these rearrangements include reciprocal chromosomal translocations, partial tandem duplications and amplification of internal coding regions [7–10]. More than 70% of infant leukaemias have translocations of the *MLL* locus on chromosome 11. MLL is fused to over 60 different partner genes, which leads to efficient transformation of haemopoietic cells into leukaemia stem cells [10]. The most frequent MLL rearrangements fuse the N-terminus of MLL to one of several components of the AFF (AF4/FMR2 family protein) 1–4 complexes, which facilitate transcription elongation. The multifunctional fusion proteins have altered stability and transcriptional activity [11]. Interestingly, even though the MLL N-terminal fusion protein MLL–AF9 does not contain the C-terminal catalytic methyltransferase domain, the wild-type allele is essential for leukaemogenesis [12]. Furthermore, reciprocal C-terminal MLL fusion proteins, such as AFF1–MLL, that retain H3K4me3 catalytic activity [13] are among the most potent leukaemogenic MLL fusions [14]. These studies suggest a role for the C-terminal catalytic SET domain in MLL-rearranged leukaemia.

Wild-type MLL functions in the context of a core multiprotein complex comprising MLL, WDR5, RbBP5 (retinoblastoma-binding protein 5) and ASH2L (absent small homoeotic discs-2-like), in which all four components are necessary for maximal enzymatic activity of H3K4 methylation [15]. The WD40 repeat proteins WDR5 and RbBP5 are essential for significant MLL activity [16], whereas ASH2L appears to stimulate maximal trimethylation of H3K4 by MLL. RbBP5/ASH2L have also been suggested to stimulate MLL activity as a heterodimer in the absence of WDR5. However, the effect was more significant at

Abbreviations used: AFF, AF4/FMR2 family protein; ASH2L, absent small homoeotic discs-2-like; DSF, differential scanning fluorimetry; HDAC, histone deacetylase; HMT, histone methyltransferase; ITC, isothermal titration calorimetry; MLL, mixed-lineage leukaemia protein; Ni-NTA, Ni^{2+}-nitrilotriacetate; PEG, poly(ethylene glycol); PTM, post-translational modification; RbBP5, retinoblastoma-binding protein 5; SET1, Su(var)3–9 enhancer-of-zeste trithorax 1; WDR5, WD40 repeat protein 5; WIN, WDR5-interacting.

[1] These authors contributed equally to this work.

[2] Correspondence may be addressed to either of these authors (email mvedadi@uhnres.utoronto.ca or carrow@uhnres.utoronto.ca).

The structures of the WDR5-01025–WDR5 and WDR5-0103–WDR5 co-crystals have been deposited in the PDB under codes 3SMR and 3UR4 respectively.

high concentrations of MLL trimeric complex [17]. WDR5 is required to maintain the integrity and activity of the MLL complex [18], as well as homologous complexes containing MLL2, MLL3 and MLL4 whose expression is often altered in other cancers [15,18–20]. WDR5 binds a conserved arginine-containing motif within MLL, the WIN (WDR5-interacting) motif, which is required for the H3K4 dimethylation activity of MLL [21,22]. Importantly, WDR5 also binds to H3 itself [16,23], recognizing Arg^2 via the same binding pocket in which the MLL WIN peptides bind [21,22]. Symmetric and asymmetric dimethylation of Arg^2 modulate the affinity of WDR5 for H3 peptides [24], and influence the H3K4 methylation activity of MLL in cells [25–27]. Importantly, WDR5 cannot bind simultaneously to both the WIN peptide (and presumably MLL) and histone 3, and the relative importance and/or regulation of these two binding events remains a mystery. A selective antagonist of the WIN/histone H3 peptide-binding site would therefore be a very useful tool for elucidating the functional role of WDR5 interactions.

Advances in understanding the mechanisms of MLL-associated leukaemias have highlighted the potential of targeting components of either the wild-type or chimaeric MLL complexes as therapeutic strategies in MLL-rearranged leukaemias [7,28]. Recently, a series of short arginine-containing peptides were shown to bind to WDR5 and disrupt its interaction with MLL [29]. In addition, peptides corresponding to the WIN motif and tight-binding histone H3 peptide mimetics were shown to inhibit the activity of the MLL core complex *in vitro* [22,30], suggesting a rationale for targeting WDR5 as a strategy to inhibit the MLL and the SET1 family of HMTs. However, in order to assess the potential of inhibiting MLL in cells or *in vivo*, it is desirable to use a cell-permeant small molecule because peptides are less effective in cells. In the present study, we have identified a small molecule that inhibits MLL HMT activity *in vitro* through disruption of the interaction of MLL with WDR5. This demonstrates proof-of-principle for pharmacological inhibition of the SET1 family of chromatin-regulatory enzymes via disruption of protein–protein interactions and serves as a starting point for further development of potential therapeutics that target WDR5-dependent complexes such as those found in MLL-rearranged leukaemias.

MATERIALS AND METHODS

Expression and purification of human MLL complex

The coding sequences of the different components of the MLL complex: WDR5 (residues 1–334), RbBP5 (residues 1–538) and MLL (residues 3745–3969) was amplified by PCR and subcloned into pFastBac™ dual vector (Invitrogen). Recombinant viral DNA generated by transformation of DH10Bac™ *Escherichia coli* cells with plasmid DNA containing the genes of interests followed by the introduction of the resulting recombinant bacmid DNA into Sf9 insect cells using Cellfectin transfection reagent (Invitrogen). Sf9 cells grown in HyQ® SFX insect serum-free medium (ThermoScientific) were co-infected with 20 ml of each required P3 viral stocks per 0.8 litre of suspension cell culture and incubated at 27 °C using a platform shaker set at 100 rev./min. The cells were collected when viability fell to 70–80 % (post-infection time varies from 48 to 72 h), washed once with ice-cold PBS. The pellet from each 0.8 litre of culture was resuspended in 40 ml of PBS containing 1× protease inhibitor cocktail (100× protease inhibitor stock in 70 % ethanol includes 0.25 mg/ml aprotinin, 0.25 mg/ml leupeptin, 0.25 mg/ml pepstatin A and 0.25 mg/ml E-64), frozen in liquid nitrogen and stored at − 80 °C. Frozen cell pellets were thawed quickly at room temperature (22 °C), and 20 μl of benzonase (250 units/μl) (Novagene), imidazole, 2-mercaptoethanol and Nonidet P40 were added to final concentrations of 5 mM, 2 mM and 0.6 % respectively. The cells were disrupted by sonication on ice for 2 min with on and off pulses at an output frequency of 8/10. The lysate was clarified by centrifugation at 21 000 rev./min for 1 h at 4 °C (Beckman Coulter, Aventi rotor JA25.50) and loaded on to a 1 ml Talon™ column (Clontech) pre-equilibrated in binding buffer (20 mM Tris/HCl, pH 7.5, 500 mM NaCl, 5 % glycerol and 5 mM imidazole) by gravity. The column was washed with 30 column volumes of binding buffer, followed by 30 column volumes of washing buffer (20 mM Tris/HCl, pH 7.5, 500 mM NaCl, 5 % glycerol and 10 mM imidazole) and the bound protein was eluted with 5 column volumes of elution buffer (20 mM Tris/HCl, pH 7.5, 500 mM NaCl, 5 % glycerol and 300 mM imidazole). The eluates were loaded on to a Superdex 200 column (26 mm diameter × 60 cm length) (GE Healthcare) pre-equilibrated in 20 mM Bis-Tris propane (pH 7.0) and 250 mM NaCl, using ÄKTA FPLC (GE Healthcare). Fractions of pure proteins were combined and concentrated for assays.

A DNA fragment encoding ASH2L (residues 1–628) was amplified by PCR and subcloned into the pET28-MHL vector, downstream of the polyhistidine coding region. The protein was expressed in *E. coli* BL21(DE3) pRARE2-V2R cells by addition of 1 mM IPTG (isopropyl β-D-thiogalactopyranoside) and incubating overnight at 15 °C. Harvested cells were resuspended in 20 mM Tris buffer (pH 7.5), supplemented with 500 mM NaCl, 5 mM imidazole and 5 % glycerol. The cells were lysed chemically followed by sonication at a frequency of 8.5 kHz for 3 min with 10 s intervals. The lysate was centrifuged and the supernatant was loaded on to DE52 pre-equilibrated high NaCl buffer, and flowthrough was loaded on to the Ni-NTA (Ni^{2+}-nitrilotriacetate) column. The column was washed with 100 ml of wash buffer (20 mM Tris/HCl, pH 7.5, 500 mM NaCl, 5 % glycerol and 50 mM imidazole) and eluted with elution buffer (same as wash buffer, but with 250 mM imidazole). TEV (tobacco etch virus) protease was added while the protein was dialysing against 20 mM Tris buffer (pH 7.5) and 500 mM NaCl, followed by removing the His_6 tag and His_6-tagged protein using the Ni-NTA column. Cut protein was loaded on a Superdex 200 column (26 mm diameter × 60 cm length) pre-equilibrated with 20 mM Tris buffer (pH 7.5) and 500 mM NaCl. Pure fractions were concentrated further and stored at − 80 °C. Tetrameric MLL complex was prepared by addition of the purified ASH2L to purified trimeric complex (Figure 1A).

Crystal structure determination

Crystallization

Purified WDR5 protein (10 mg/ml) was mixed with WDR5-0102 or WDR5-0103 at a 1:5 molar ratio of protein to compound and crystallized using the sitting-drop vapour-diffusion method by adding 1 μl of protein solution to 1 μl of the reservoir solution containing 25 % PEG [poly(ethylene glycol)] 3350, 0.2 M ammonium acetate, 0.1 M BisTris (pH 6.5), and 22 % PEG3350, 0.1 M ammonium sulfate and 0.1 M BisTris (pH 6.0) respectively. Crystals were soaked in the corresponding mother liquor supplemented with 20 % ethylene glycol as cryoprotectant before freezing in liquid nitrogen.

Data collection and processing

Diffraction data for crystals of WDR5 in complex with WDR5-0102 and WDR5-0103 were collected on a Rigaku FR-E

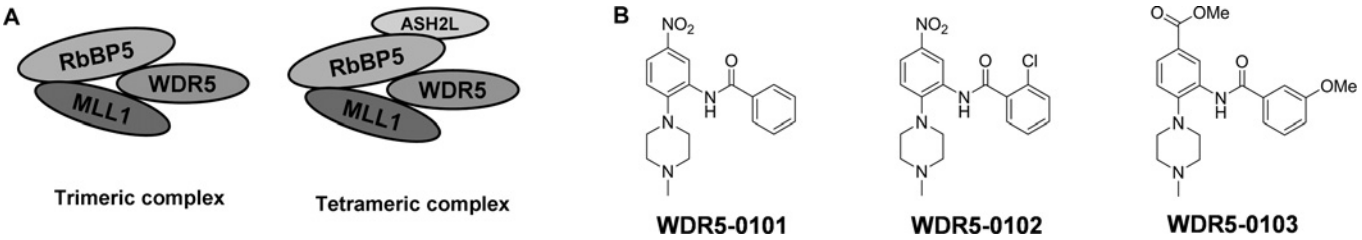

Figure 1 MLL complex and WDR5 binders

(**A**) Trimeric and tetrameric MLL complexes [42]. (**B**) WDR5 antagonists: WDR5-0101 [*N*-(2-(4-methylpiperazin-1-yl)-5 nitrophenyl)benzamide], WDR5-0102 [2-chloro-*N*-(2-(4-methylpiperazin-1-yl)-5-nitrophenyl) benzamide] and WDR5-0103 [methyl-3-(3-methoxybenzamido)-4-(4-methylpiperazin-1-yl)benzoate] were identified as ligands for WDR5.

SuperBright instrument. For WDR5 in complex with WDR5-0102, the data were collected on a Rigaku R-AXIS HTC instrument, and for WDR5 in complex with WDR5-0103, the data were collected on a Rigaku Saturn A200 CCD (charge-coupled device) detector. The program suite HKL3000 was used to integrate and scale both datasets [31].

Structure determination and refinement

Both WDR5 co-crystal structures were determined by molecular replacement using the PDB code 2O9K model as the search template. The graphic program Coot [32] was used for manual model refinement and visualization. Refmac5 [33] was used to refine the model. MolProbity [34] was used to validate the refined structure; 96.1 % residues are in the favoured regions of the Ramachandran plot. The structures have been deposited in the PDB under codes 3SMR and 3UR4 respectively. Crystal diffraction data and refinement statistics for the structures are shown in Supplementary Table S1 at http://www.biochemj.org/bj/449/bj4490151add.htm. Supplementary Figure S1 (at http://www.biochemj.org/bj/449/bj4490151add.htm) also provides omit maps of electron density for WDR5-0102 and WDR5-0103.

Commercial expansion around WDR5-0101

Analogues of WDR5-0101 were identified in a database of over six million unique commercial molecules using MolCart version 2010 (Molsoft). First, the compound was used as a substructure query to search for larger analogues. Secondly, a fingerprint similarity search was conducted using the compound as a query with maximum Tanimoto distance of 0.2 to WDR5-0101. Thirdly, the nitro group was truncated from WDR5-0101, and the resulting fragment was used as a substructure search query to retrieve larger analogues. Hits from the three searches were merged, duplicates were removed and derivatives that had already been screened in the 16 000 compound library were discarded. The resulting 1358 compounds were clustered using ICM (Molsoft). A total of 119 compounds were selected, purchased and assayed.

Compound quality control

Compounds ordered from vendors were evaluated for purity by LC (liquid chromatography)–MS with an acceptable purity standard set at $\geqslant$85 % by UV (254 nm). Purity (along with compound identity) was assessed further by NMR spectroscopy (500 MHz), and compounds failing to meet the standard were subsequently purified by silica gel column chromatography before further assessment.

Binding assays

Fluorescence polarization

The MLL–WIN (GSARAEVHLRKS) peptide for WDR5 was synthesized, N-terminally labelled with FITC and purified by Tufts University Core Services (Boston, MA, U.S.A.). Compound binding assays were performed in a 10 μl volume at a constant labelled peptide concentration of 40 nM and protein concentration of 5 μM WDR5. The assay buffer was 100 mM potassium phosphate (pH 8.0), 150 mM NaCl and 0.01 % Triton X-100. Fluorescence polarization assays were performed in 384-well Axygen plates using a Synergy 2 microplate reader (BioTek). An excitation wavelength of 485 nm and an emission wavelength of 528 nm were used.

DSF (differential scanning fluorimetry)

DSF measurements were performed with a Light Cycler 480 II instrument from Roche Applied Science. The protein solutions used for all fluorescence measurements employed a final protein concentration of 0.1 mg/ml in a buffer consisting of 0.1 M Hepes (pH 7.5) and 0.15 M NaCl. Sypro Orange, purchased from Invitrogen as a 5000× stock solution was diluted 1:1000 to yield a 5× working concentration. Invitrogen does not specify the concentration. Different concentrations of compounds were included as needed. DSF was carried out by increasing the temperature by 1 °C/min from 20 to 95 °C, and data points were collected at 1 °C intervals. The temperature scan curves were fitted to a Boltzmann sigmoid function, and the T_m values were obtained from the midpoint of the transition as described previously [35].

ITC (isothermal titration calorimetry)

Purified WDR5 was dialysed in ITC buffer (100 mM Hepes, pH 7.5, and 150 mM NaCl). Compounds at 0.2 mM for WDR5-0103 and 0.5 mM for WDR5-0101 and WDR5-0102 were injected into the sample cell containing approximately 1.4 ml of 25 μM WDR5. ITC titrations were performed on a VP-ITC MicroCalorimeter from GE Healthcare at 25 °C by using 10 μl injection with a total of 25 injections. Data were fitted with a one-binding site model using Microcal Origin software.

Enzyme assays

The effect of WDR5-0103 on the activity of the MLL complex was tested in at least duplicate at three different concentrations of trimeric (125, 500 and 1000 nM) and tetrameric (10, 50 and 125 nM) MLL complex. Reactions were carried out in 20 μl of 20 mM Tris/HCl (pH 8.0), 5 mM DTT (dithiothreitol)

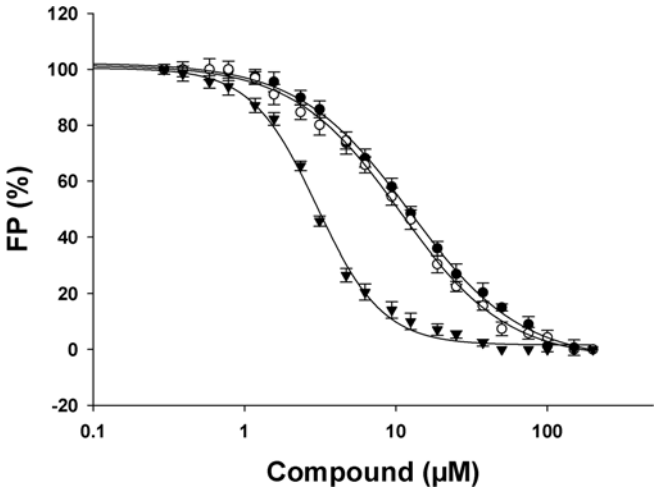

Figure 2 Assessing the binding affinity of compounds by peptide displacement

Binding affinity of WDR5-0101 (●), WDR5-0102 (○) and WDR5-0103 (▼) were assessed by peptide displacement monitoring decrease in fluorescence polarization (FP) signal. Results are means ± S.D. of triplicate measurements.

and 0.01 % Triton X-100 in the presence of 2 μM [^{3}H]SAM (*S*-adenosylmethionine) and 5 μM of biotinylated H3 (1–25) peptide. For IC_{50} determinations, reaction mixtures with various concentrations of WDR5-0103 (1 μM–1 mM) were incubated for 1 h at room temperature and then quenched by adding 20 μl of 7.5 M guanidinium chloride, followed by the addition of 180 μl of buffer (20 mM Tris/HCl, pH 8.0). The reactions were mixed and transferred to a streptavidin-coated 96-well microplate (FlashPlate from PerkinElmer). The FlashPlates were incubated for at least 1 h and the c.p.m. values were determined using a Topcount plate reader. The IC_{50} values were determined using SigmaPlot software.

RESULTS

Identification of WDR5-binding small molecules

To identify compounds that disrupt the WDR5–MLL interaction (Figure 1A), we established an assay to detect displacement of a fluorescein-labelled WIN peptide (GSARAEVHLRKS) from its binding pocket in WDR5 using fluorescence polarization [36]. We screened a library of 16 000 diverse small molecules (see the Supplementary Online Data http://www.biochemj.org/bj/449/bj4490151add.htm) at an initial compound concentration of 50 μM, and identified 17 compounds with greater than 40 % displacement (0.1 % hit rate). All 17 compounds were titrated over a range of concentrations from 0 to 100 μM, and only compound WDR5-0101 (Figure 1B) displaced the WIN peptide with a K_{dis} ($K_{displacement}$) of less than 60 μM (Figure 2 and Table 1) (K_{dis} 12 ± 1 μM).

In an attempt to identify analogues of WDR5-0101 that bind to WDR5 with higher affinity, we searched a database of over 6 million unique commercially available compounds for those with similar chemical structures. A total of 119 compounds were selected, purchased and screened in the peptide-displacement assay. Of these, WDR5-0102 and WDR5-0103 (Figure 1B and Table 1) showed promising K_{dis} values (11 ± 1 and 3.0 ± 0.1 μM respectively).

Direct binding of WDR5-0101, WDR5-0102 and WDR5-0103 to WDR5 was assessed by DSF (Figure 3 and Table 1) yielding ΔT_m values of 3.8 ± 0.1, 4.8 ± 0.1 and 8.4 ± 0.1 °C respectively. ITC experiments also confirmed the binding of all three compounds, and WDR5-0103 had the lowest K_d value (0.45 μM) (Figure 4 and Table 1).

Table 1 Binding affinity of compounds

Binding affinity of WDR5-0101, WDR5-0102 and WDR5-0103 were assessed by DSF, ITC and peptide displacement monitored by fluorescence polarization. ΔT_m values were determined for 100 μM compounds by DSF (Figure 3). K_d and K_{dis} values were determined by ITC and fluorescence polarization (peptide displacement) respectively. Experiments were performed in triplicate.

Compound	ΔT_m (°C)	K_d (μM)	K_{dis} (μM)
WDR5-0101	3.8 ± 0.1	5.5 ± 0.6	12 ± 1
WDR5-0102	4.8 ± 0.1	4.0 ± 1.1	11 ± 1
WDR5-0103	8.4 ± 0.1	0.45 ± 0.02	3.0 ± 0.1

Structural basis of WDR5 inhibition

To better understand the nature of the interaction of these compounds with WDR5, we determined the crystal structures of WDR5-0102 and WDR5-0103 in complex with WDR5 (PDB codes 3SMR and 3UR4 respectively; Supplementary Table S1). Similar to previous peptide-bound structures, WDR5 adopts a doughnut-shaped WD40-repeat fold with a deep central cavity that normally accommodates an arginine side chain of interacting peptides [21–23,37,38]. WDR5-0102-bound WDR5 has a backbone RMSD (root mean square deviation) of 0.4 Å (1 Å = 0.1 nm) relative to the structure of WDR5 in complex with MLL and RbBP5 peptides [37] and binds in the central cavity within the arginine-binding pocket (Figure 5A). WDR5-0102 therefore competes directly with, and antagonizes the binding of, partner peptides or proteins within the central cavity of WDR5. To the best of our knowledge, the only other non-peptide WD40-repeat small-molecule antagonist reported to date is an inhibitor of yeast Cdc4, that intercalates between two WD40 blades on the outer edge of the WD40 structure [39] (Figure 5A).

The amide group of WDR5-0102 forms one direct and one water-mediated hydrogen bond with the side chain of Ser^{91} and the backbone nitrogen of Cys^{261} respectively. The *N*-methylpiperazine moiety, predicted to be mainly protonated at physiological pH, is anchored at the bottom of the pocket, at a site occupied by the critical arginine residue from the MLL and histone H3 peptides [37,38], and forms a water-mediated hydrogen bond with the backbone carbonyl of Cys^{261} (Figure 5B). The 2-chlorophenyl group lies in a shallow, mostly hydrophobic, cavity that is also occupied by H3 and MLL peptides, and is surrounded by Leu^{321}, Ala^{47} and the aliphatic section of Ser^{49} and Ser^{91} side chains. Surprisingly, the nitroaryl group occupies a section of the cleft that is occluded in most WDR5 structures, but is open in the WDR5-0102-bound structure owing to flipping of Phe^{133} and Phe^{149} side chains (Figure 5C). This additional hydrophobic cavity is not present in H3- or MLL-bound structures (PDB codes 2CNX and 3EMH respectively) [38,40]. At the bottom of the pocket, Phe^{263} is also flipped in a previously unseen rotameric state to accommodate the piperazine moiety of the antagonist (Figure 5C). These structural variations reveal an unforeseen pharmacophore profile for the chemical antagonism of WDR5.

WDR5-0103 occupies the binding pocket with a similar geometry to that of WDR5-0102, but the methoxy substituent induces a 2.5 Å shift of the benzamide ring in the upper shallow

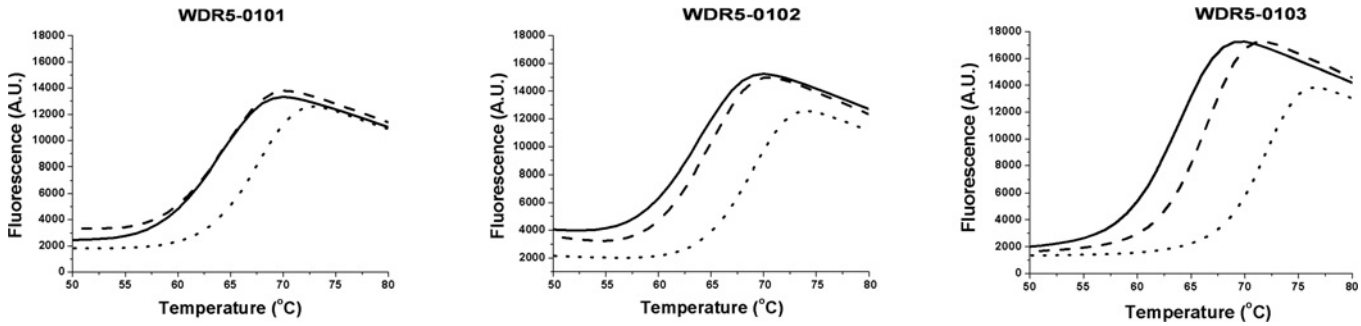

Figure 3 Assessing the binding affinity of compounds by DSF

Binding of WDR5-0101, WDR5-0102 and WDR5-0103 were monitored by DSF at 0 (—), 6 μM (- -) and 100 μM (···) of compound. A.U., arbitrary units.

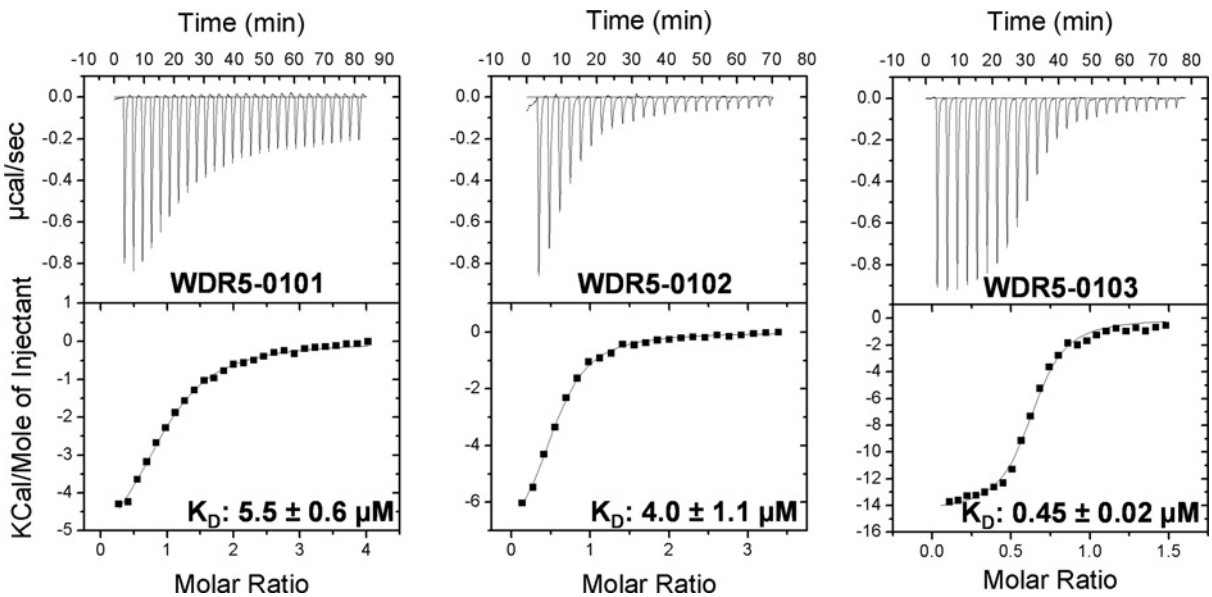

Figure 4 Assessing the binding affinity of compounds by ITC

Binding of WDR5-0101, WDR5-0102 and WDR5-0103 were assessed by ITC as described in the Materials and methods section.

region of the pocket, which is accompanied by a motion of the amide linker and flipping of the Ser[91] side chain (Figures 5D and 5E). The increased potency of WDR5-0103 is in agreement with improved occupancy of the shallow pocket by the methoxy group, and of the hydrophobic groove between Tyr[191] and Phe[149] by the ester moiety (Figure 5F).

Inhibition of methyltransferase activity of MLL complex *in vitro*

To investigate whether WDR5-0103 can inhibit the methyltransferase activity of a pre-formed MLL–WDR5–RbBP5 core complex (trimeric complex; Figure 1A) *in vitro*, we determined the IC_{50} values for WDR5-0103 at various concentrations of the trimeric protein complex (Figure 6A). At an MLL complex concentration of 0.125 μM, WDR5-0103 inhibited MLL catalytic activity with an IC_{50} value of 39 ± 10 μM. An increase in MLL complex concentration resulted in proportional increase in IC_{50} values for WDR5-0103 (83 ± 10 and 280 ± 12 μM at concentrations of 500 and 1000 nM of the core trimeric MLL complex respectively). These data are consistent with a mechanism of action in which WDR5-0103 antagonizes the interaction of WDR5 with MLL by competing with MLL for their mutual binding site on WDR5. At concentrations of MLL complex above the K_d of the MLL–WDR5 interaction (>120 nM) [21] increasing amounts of WDR5-0103 are required to displace WDR5. We also assessed the effect of WDR5-0103 on the activity of pre-formed MLL–WDR5–RbBP5–ASH2L complex at 10, 50 and 125 nM enzyme (Figure 6B). The tetrameric complex was significantly more active than the trimeric complex which does not include ASH2L (k_{cat} values of 27 ± 0.3 compared with 3.4 ± 0.1 h^{-1}; Supplementary Figure S2 and Supplementary Table S2 at http://www.biochemj.org/bj/449/bj4490151add.htm). The tetrameric complex appeared to be more stable and, overall, the WDR5-0103 effect was less pronounced. However, similar to the trimeric complex, the inhibitory effect on the tetrameric complex was diminished with increasing protein concentration (Figure 6B).

In order to confirm that WDR5-0103 is not a promiscuous compound, we tested its inhibitory activity on a panel of other human HMTs. At concentrations up to 100 μM, WDR5-0103 showed no inhibitory effect on the human H3K4 methyltransferase SETD7, or six other HMTs (G9a, EHMT1, SUV39H2, SETD8, PRMT3 and PRMT5) (Supplementary Figure S3 at http://www.biochemj.org/bj/449/bj4490151add.htm). These results highlight the specificity of the molecule for the MLL complex.

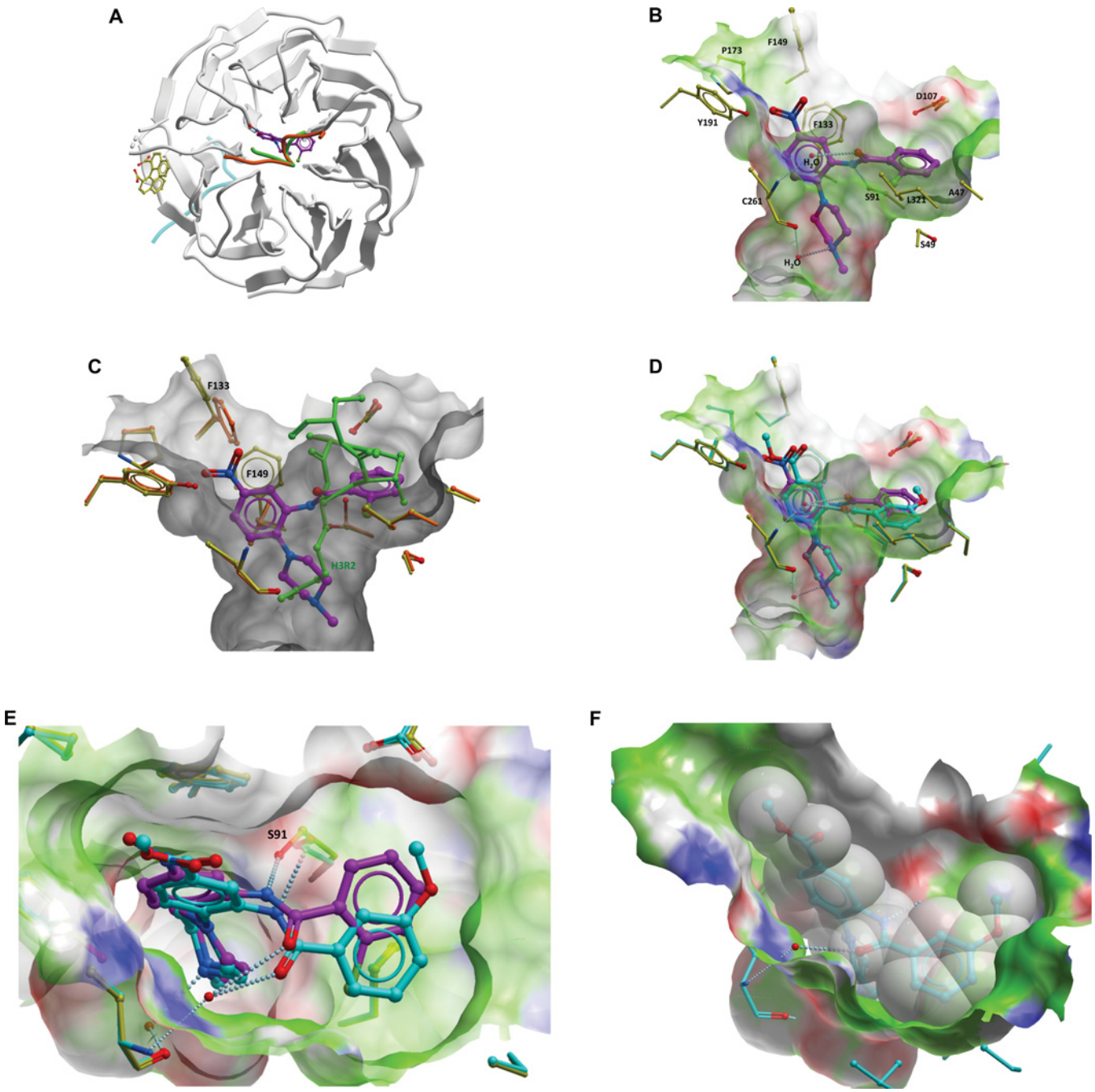

Figure 5 Structural mechanism of inhibition

(**A**) WDR5 co-crystallized with WDR5-0102 was superimposed with (i) a WDR5 ternary structure in complex with an MLL peptide (orange) and a RbBP5 peptide (cyan) [37], (ii) a WDR5 binary structure in complex with a histone H3 peptide (green) [38], and (iii) the yeast WD40 repeat protein Cdc4 in complex with an allosteric inhibitor (shown in yellow) [39]. WDR5-0102 (magenta) occupies the central cavity of the canonical WD40 repeat structure that acts as a recruitment site for MLL and H3. (**B**) The amide and *N*-methylpiperazine groups of WDR5-0102 form three direct or water-mediated hydrogen bonds with WDR5. The 2-chlorophenyl and nitroaryl groups are mostly surrounded with hydrophobic side chains. Molecular surface colour-code is green, hydrophobic; red, hydrogen-bond acceptor; blue, hydrogen-bond donor. Sticks colour code is blue, nitrogen; red, oxygen; green, chlorine. (**C**) Superimposing WDR5 in complex with WDR5-0102 (WDR5, yellow; WDR5-0102, magenta) and in complex with an N-acetylated histone H3 tetrapeptide (WDR5, orange; histone H3, green) shows that the *N*-methylpiperazine maps at the site occupied by the histone H3 Arg^2 side chain [30]. The nitroaryl group exploits a hydrophobic cavity that is occluded in most WDR5 structures, owing to the inward collapse of surrounding Phe^{133} and Phe^{149} side chains. (**D**) WDR5-0102 (magenta) and WDR5-0103 (cyan) adopt a similar pose in the WDR5-binding pocket. (**E**) Shifting motion of the amide axis can be induced by diverse substituants on the benzamide ring. (**F**) The methoxyphenyl and ester groups of WDR5-0103 increase shape complementarity with the binding pocket.

DISCUSSION

The literature describing the role of WDR5 activation of MLL catalytic activity is complex and sometimes contradictory. WDR5 has been reported to (i) directly mediate formation of the tetrameric core complex [15], (ii) facilitate interaction of the MLL1 catalytic subunit with the histone substrate [15,38,41], and (iii) contribute to formation of a stable complex with RbBP5 and

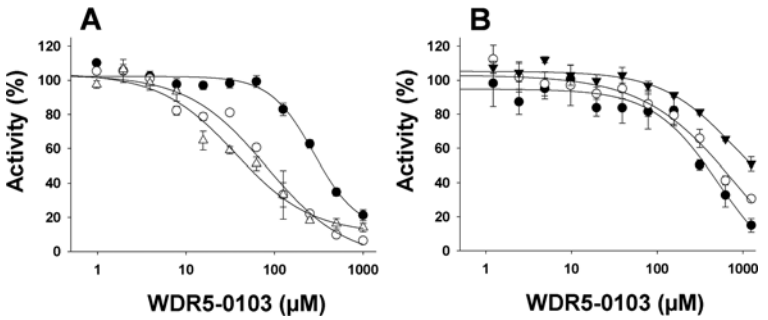

Figure 6 Effect of WDR5-0103 on MLL complex activity

Effect of WDR5-0103 on activity of (**A**) trimeric MLL complex at concentrations of (△) 125, (○) 500 and (●) 1000 nM, and (**B**) tetrameric MLL complex at concentrations of (●) 10, (○) 50 and (▼) 125 nM were assessed. IC_{50} values of 39 ± 10, 83 ± 10 and 280 ± 12 μM were determined at 125, 500 and 1000 nM of trimeric MLL complex respectively. IC_{50} values for WDR5-0103 and the tetrameric MLL complex were significantly higher and were not calculated owing to incomplete fitting. However, the inhibitory effect of WDR5-0103 is more pronounced as the concentration of tetrameric MLL complex was lowered to 10 nM. Results are means $\pm$ S.D. of quadruplicate measurements.

ASH2L in the absence of MLL-C [15,42]. WDR5 was also shown to be essential for the ASH2L-mediated trimethylation activity of MLL [18]. Within the core complex, WDR5 was reported to bind tightly (K_d of 120 nM) to the MLL catalytic subunit and is essential for MLL complex formation and activation [43]. Other reports indicated that WDR5 alone has no significant effect in activating MLL, whereas RbBP5 and ASH2L–Dpy30 can activate MLL in the absence of WDR5 [42,44]. However, there is a consensus on the critical role of WDR5 for maintaining the integrity of the complex and fully activating the MLL catalytic potential through interaction with other components of the complex [42]. In the absence of WDR5, neither RbBP5 nor ASH2L has a stable interaction with MLL [15,44]. WDR5 interaction with the WIN motif of MLL through Arg^{3765} of MLL has been shown to be essential for complex assembly and resultant H3K4 methylation [18,22]. WDR5 is also an essential component of other SET1-containing complexes that methylate H3K4 [15,18,20].

In order to better understand the functional role of WDR5's mutually exclusive interactions with the WIN motif of MLL and histone H3 N-terminal peptides, we sought to identify a small-molecule antagonist of the WDR5–WIN/histone H3 peptide interactions. In the present study, we show that WDR5-0103 effectively antagonizes the WDR5–WIN peptide interaction and compromises the catalytic activity of the MLL-C trimeric and tetrameric complexes *in vitro*. Interestingly, the effect of WDR5-0103 on both MLL-C complexes is dependent on protein concentration. These results are consistent with a direct stabilization of the MLL complex via WDR5's interaction with the WIN motif of MLL. This model is also supported by observations that the effect of WDR5 on the activity of the MLL-C–RbBP5–ASH2L complex is also protein-concentration-dependent [17]. The cellular concentrations of the MLL complex are likely to be within the lower range of protein concentrations used in the present study. It is therefore reasonable to expect that more potent and cell-permeant compounds could effectively antagonize the cellular activity of MLL and possibly other WDR5-dependent SET1 family enzymes.

Further optimization of WDR5-0103 may be possible. WDR5-0103 appears to be reasonably selective, as it did not affect methyltransferase activity of the seven HMTs tested, including SETD7, a WDR5-independent H3K4 HMT. Our structural data highlight several features of the WDR5-binding cavity that can be exploited to design in greater potency and cell permeability. For example, the carboxy side chain of Asp^{107} at the rim of the pocket, or the backbone carbonyl oxygens of Ser^{49}, Ser^{91}, Phe^{133} and Cys^{261} directly surrounding the piperazine moiety at the bottom of the pocket are not exploited by WDR5-0103.

Our data indicate that WDR5 appears to be a druggable target whose antagonism can modulate the activity of an important epigenetic enzyme. The plasticity of the WDR5 arginine-binding pocket allows binding to the WIN motifs of MLL2, MLL3, MLL4, SET1A and SET1B enzymes which play an important role in their methyltransferase activity [45]. WDR5 antagonists may also affect the activity of these members of the SET1 family of PKMTs (protein lysine/arginine methyltransferases). Assessment of the full potential of WDR5 as a therapeutic target for cancer or other diseases will probably require a more potent compound coupled with detailed phenotypic and mechanistic studies to elucidate the functions of the multiple WDR5-dependent protein complexes. For example, WDR5 was recently shown to be induced by hypoxia, leading to increased H3K4me3 levels at mesenchymal genes, and together with HDAC (histone deacetylase) 3 was essential for hypoxia-induced epithelial–mesenchymal transition [46]. Thus WDR5 antagonists may be synergistic with HDAC inhibitors in certain cancers, in addition to their potential for MLL-rearranged leukaemia or solid tumours with overexpression of MLL2 or MLL3. Our results establish a basis for further exploration and development of WDR5 antagonists.

AUTHOR CONTRIBUTION

Guillermo Senisterra and Gregory Wasney performed screening and follow-up confirmation experiments (Figures 1B and 2), Guillermo Senisterra also performed DSF and ITC experiments (Figures 3 and 4). Abdellah Allali-Hassani developed and performed MLL activity assays (Figure 6, Supplementary Figure S2 and Supplementary Table S2). Hong Wu and Ludmila Dombrovski purified and co-crystallized WDR5 and compounds. Aiping Dong determined the crystal structure of WDR5 in complex with both compounds (Supplementary Figure S1 and Supplementary Table S1). Hao He and Alma Seitova expressed proteins in a baculovirus system. Taraneh Hajian and Irene Chau purified WDR5 and MLL complexes for screening, as well as purifying all other proteins used to determine selectivity. Fengling Li performed all selectivity assays (Supplementary Figure S3). Matthieu Schapira and Kong Nguyen performed hit expansion. Matthieu Schapira performed structural analysis (Figure 5) and wrote the paper. Rima Al-awar and Gennadiy Poda provided the initial library of compounds. David Smil and Yuri Bolshan performed compound quality control experiments. Rima Al-awar, Gennadiy Poda, Peter Brown, Dalia Barsyte-Lovejoy and Jean-François Couture contributed to experimental design and editing of the paper before submission. Masoud Vedadi and Cheryl Arrowsmith reviewed data, contributed to experimental design and wrote the paper. Masoud Vedadi was the principal investigator, designed experiments, analysed data and supervised the screening and hit confirmation process.

ACKNOWLEDGEMENT

We thank Dr Aled Edwards for a critical review of the paper before submission.

FUNDING

The Structural Genomics Consortium is a registered charity (number 1097737) that receives funds from Canadian Institutes of Health Research, Eli Lilly Canada, Genome Canada, GlaxoSmithKline, the Ontario Ministry of Economic Development and Innovation, the Novartis Research Foundation, Pfizer, AbbVie, Takeda and the Wellcome Trust. C.H.A. holds a Canada Research Chair in Structural Genomics. Funding for OICR (Ontario Institute for Cancer Research) is provided by the Ontario Ministry of Economic Development and Innovation.

REFERENCES

1 Jenuwein, T. and Allis, C. D. (2001) Translating the histone code. Science **293**, 1074–1080
2 Rice, J. C. and Allis, C. D. (2001) Histone methylation versus histone acetylation: new insights into epigenetic regulation. Curr. Opin. Cell Biol. **13**, 263–273
3 Trievel, R. C. and Shilatifard, A. (2009) WDR5, a complexed protein. Nat. Struct. Mol. Biol. **16**, 678–680
4 Argiropoulos, B. and Humphries, R. K. (2007) Hox genes in hematopoiesis and leukemogenesis. Oncogene **26**, 6766–6776
5 Rampalli, S., Li, L., Mak, E., Ge, K., Brand, M., Tapscott, S. J. and Dilworth, F. J. (2007) p38 MAPK signaling regulates recruitment of Ash2L-containing methyltransferase complexes to specific genes during differentiation. Nat. Struct. Mol. Biol. **14**, 1150–1156
6 Lim, D. A., Huang, Y. C., Swigut, T., Mirick, A. L., Garcia-Verdugo, J. M., Wysocka, J., Ernst, P. and Alvarez-Buylla, A. (2009) Chromatin remodelling factor Mll1 is essential for neurogenesis from postnatal neural stem cells. Nature **458**, 529–533
7 Liedtke, M. and Cleary, M. L. (2009) Therapeutic targeting of MLL. Blood **113**, 6061–6068
8 Tkachuk, D. C., Kohler, S. and Cleary, M. L. (1992) Involvement of a homolog of *Drosophila trithorax* by 11q23 chromosomal translocations in acute leukemias. Cell **71**, 691–700
9 Gu, Y., Nakamura, T., Alder, H., Prasad, R., Canaani, O., Cimino, G., Croce, C. M. and Canaani, E. (1992) The t(4;11) chromosome translocation of human acute leukemias fuses the ALL-1 gene, related to *Drosophila trithorax*, to the *AF-4* gene. Cell **71**, 701–708
10 Krivtsov, A. V. and Armstrong, S. A. (2007) MLL translocations, histone modifications and leukaemia stem-cell development. Nat. Rev. Cancer **7**, 823–833
11 Marschalek, R. (2011) Mechanisms of leukemogenesis by MLL fusion proteins. Br. J. Haematol. **152**, 141–154
12 Thiel, A. T., Blessington, P., Zou, T., Feather, D., Wu, X., Yan, J., Zhang, H., Liu, Z., Ernst, P., Koretzky, G. A. and Hua, X. (2010) MLL-AF9-induced leukemogenesis requires coexpression of the wild-type Mll allele. Cancer Cell **17**, 148–159
13 Benedikt, A., Baltruschat, S., Scholz, B., Bursen, A., Arrey, T. N., Meyer, B., Varagnolo, L., Muller, A. M., Karas, M., Dingermann, T. and Marschalek, R. (2011) The leukemogenic AF4–MLL fusion protein causes P-TEFb kinase activation and altered epigenetic signatures. Leukemia **25**, 135–144
14 Bursen, A., Schwabe, K., Ruster, B., Henschler, R., Ruthardt, M., Dingermann, T. and Marschalek, R. (2010) The AF4·MLL fusion protein is capable of inducing ALL in mice without requirement of MLL·AF4. Blood **115**, 3570–3579
15 Dou, Y., Milne, T. A., Ruthenburg, A. J., Lee, S., Lee, J. W., Verdine, G. L., Allis, C. D. and Roeder, R. G. (2006) Regulation of MLL1 H3K4 methyltransferase activity by its core components. Nat. Struct. Mol. Biol. **13**, 713–719
16 Wysocka, J., Swigut, T., Milne, T. A., Dou, Y., Zhang, X., Burlingame, A. L., Roeder, R. G., Brivanlou, A. H. and Allis, C. D. (2005) WDR5 associates with histone H3 methylated at K4 and is essential for H3 K4 methylation and vertebrate development. Cell **121**, 859–872
17 Cao, F., Chen, Y., Cierpicki, T., Liu, Y., Basrur, V., Lei, M. and Dou, Y. (2010) An Ash2L/RbBP5 heterodimer stimulates the MLL1 methyltransferase activity through coordinated substrate interactions with the MLL1 SET domain. PLoS ONE **5**, e14102
18 Steward, M. M., Lee, J. S., O'Donovan, A., Wyatt, M., Bernstein, B. E. and Shilatifard, A. (2006) Molecular regulation of H3K4 trimethylation by ASH2L, a shared subunit of MLL complexes. Nat. Struct. Mol. Biol. **13**, 852–854
19 Huntsman, D. G., Chin, S. F., Muleris, M., Batley, S. J., Collins, V. P., Wiedemann, L. M., Aparicio, S. and Caldas, C. (1999) MLL2, the second human homolog of the *Drosophila trithorax* gene, maps to 19q13.1 and is amplified in solid tumor cell lines. Oncogene **18**, 7975–7984
20 Cho, Y. W., Hong, T., Hong, S., Guo, H., Yu, H., Kim, D., Guszczynski, T., Dressler, G. R., Copeland, T. D., Kalkum, M. and Ge, K. (2007) PTIP associates with MLL3- and MLL4-containing histone H3 lysine 4 methyltransferase complex. J. Biol. Chem. **282**, 20395–20406
21 Patel, A., Dharmarajan, V. and Cosgrove, M. S. (2008) Structure of WDR5 bound to mixed lineage leukemia protein-1 peptide. J. Biol. Chem. **283**, 32158–32161
22 Patel, A., Vought, V. E., Dharmarajan, V. and Cosgrove, M. S. (2008) A conserved arginine-containing motif crucial for the assembly and enzymatic activity of the mixed lineage leukemia protein-1 core complex. J. Biol. Chem. **283**, 32162–32175
23 Schuetz, A., Allali-Hassani, A., Martin, F., Loppnau, P., Vedadi, M., Bochkarev, A., Plotnikov, A. N., Arrowsmith, C. H. and Min, J. (2006) Structural basis for molecular recognition and presentation of histone H3 by WDR5. EMBO J. **25**, 4245–4252
24 Migliori, V., Muller, J., Phalke, S., Low, D., Bezzi, M., Mok, W. C., Sahu, S. K., Gunaratne, J., Capasso, P., Bassi, C. et al. (2012) Symmetric dimethylation of H3R2 is a newly identified histone mark that supports euchromatin maintenance. Nat. Struct. Mol. Biol. **19**, 136–144
25 Hyllus, D., Stein, C., Schnabel, K., Schiltz, E., Imhof, A., Dou, Y., Hsieh, J. and Bauer, U. M. (2007) PRMT6-mediated methylation of R2 in histone H3 antagonizes H3 K4 trimethylation. Genes Dev. **21**, 3369–3380
26 Guccione, E., Bassi, C., Casadio, F., Martinato, F., Cesaroni, M., Schuchlautz, H., Luscher, B. and Amati, B. (2007) Methylation of histone H3R2 by PRMT6 and H3K4 by an MLL complex are mutually exclusive. Nature **449**, 933–937
27 Iberg, A. N., Espejo, A., Cheng, D., Kim, D., Michaud-Levesque, J., Richard, S. and Bedford, M. T. (2008) Arginine methylation of the histone H3 tail impedes effector binding. J. Biol. Chem. **283**, 3006–3010
28 Muntean, A. G. and Hess, J. L. (2012) The pathogenesis of mixed-lineage leukemia. Annu. Rev. Pathol. **7**, 283–301
29 Karatas, H., Townsend, E. C., Bernard, D., Dou, Y. and Wang, S. (2010) Analysis of the binding of mixed lineage leukemia 1 (MLL1) and histone 3 peptides to WD repeat domain 5 (WDR5) for the design of inhibitors of the MLL1–WDR5 interaction. J. Med. Chem. **53**, 5179–5185
30 Avdic, V., Zhang, P., Lanouette, S., Voronova, A., Skerjanc, I. and Couture, J. F. (2011) Fine-tuning the stimulation of MLL1 methyltransferase activity by a histone H3-based peptide mimetic. FASEB J. **25**, 960–967
31 Minor, W., Cymborowski, M., Otwinowski, Z. and Chruszcz, M. (2006) HKL-3000: the integration of data reduction and structure solution: from diffraction images to an initial model in minutes. Acta Crystallogr. Sect. D Biol. Crystallogr. **62**, 859–866
32 Emsley, P. and Cowtan, K. (2004) Coot: model-building tools for molecular graphics. Acta Crystallogr. Sect. D Biol. Crystallogr. **60**, 2126–2132
33 Murshudov, G. N., Vagin, A. A. and Dodson, E. J. (1997) Refinement of macromolecular structures by the maximum-likelihood method. Acta Crystallogr. Sect. D Biol. Crystallogr. **53**, 240–255
34 Chen, V. B., Arendall, W. B., Headd, J. J., Keedy, D. A., Immormino, R. M., Kapral, G. J., Murray, L. W., Richardson, J. S. and Richardson, D. C. (2010) MolProbity: all-atom structure validation for macromolecular crystallography. Acta Crystallogr. Sect. D Biol. Crystallogr. **66**, 12–21
35 Vedadi, M., Niesen, F. H., Allali-Hassani, A., Fedorov, O. Y., Finerty, Jr, P. J., Wasney, G. A., Yeung, R., Arrowsmith, C., Ball, L. J., Berglund, H. et al. (2006) Chemical screening methods to identify ligands that promote protein stability, protein crystallization, and structure determination. Proc. Natl. Acad. Sci. U.S.A. **103**, 15835–15840
36 Allali-Hassani, A., Wasney, G. A., Siarheyeva, A., Hajian, T., Arrowsmith, C. H. and Vedadi, M. (2011) Fluorescence-based methods for screening writers and readers of histone methyl marks. J. Biomol. Screen. **17**, 71–84
37 Avdic, V., Zhang, P., Lanouette, S., Groulx, A., Tremblay, V., Brunzelle, J. and Couture, J. F. (2011) Structural and biochemical insights into MLL1 core complex assembly. Structure **19**, 101–108
38 Ruthenburg, A. J., Wang, W., Graybosch, D. M., Li, H., Allis, C. D., Patel, D. J. and Verdine, G. L. (2006) Histone H3 recognition and presentation by the WDR5 module of the MLL1 complex. Nat. Struct. Mol. Biol. **13**, 704–712
39 Orlicky, S., Tang, X., Neduva, V., Elowe, N., Brown, E. D., Sicheri, F. and Tyers, M. (2010) An allosteric inhibitor of substrate recognition by the SCF(Cdc4) ubiquitin ligase. Nat. Biotechnol. **28**, 733–737
40 Song, J. J. and Kingston, R. E. (2008) WDR5 interacts with mixed lineage leukemia (MLL) protein via the histone H3-binding pocket. J. Biol. Chem. **283**, 35258–35264
41 Han, Z., Guo, L., Wang, H., Shen, Y., Deng, X. W. and Chai, J. (2006) Structural basis for the specific recognition of methylated histone H3 lysine 4 by the WD-40 protein WDR5. Mol. Cell **22**, 137–144
42 Odho, Z., Southall, S. M. and Wilson, J. R. (2010) Characterization of a novel WDR5-binding site that recruits RbBP5 through a conserved motif to enhance methylation of histone H3 lysine 4 by mixed lineage leukemia protein-1. J. Biol. Chem. **285**, 32967–32976

43 Patel, A., Dharmarajan, V., Vought, V. E. and Cosgrove, M. S. (2009) On the mechanism of multiple lysine methylation by the human mixed lineage leukemia protein-1 (MLL1) core complex. J. Biol. Chem. **284**, 24242–24256
44 Southall, S. M., Wong, P. S., Odho, Z., Roe, S. M. and Wilson, J. R. (2009) Structural basis for the requirement of additional factors for MLL1 SET domain activity and recognition of epigenetic marks. Mol. Cell **33**, 181–191
45 Zhang, P., Lee, H., Brunzelle, J. S. and Couture, J. F. (2012) The plasticity of WDR5 peptide-binding cleft enables the binding of the SET1 family of histone methyltransferases. Nucleic Acids Res. **40**, 4237–4246
46 Wu., M. Z., Tsai, Y. P., Yang, M. H., Huang, C. H., Chang, S. Y., Chang, C. C., Teng, S. C. and Wu, K. J. (2011) Interplay between HDAC3 and WDR5 is essential for hypoxia-induced epithelial–mesenchymal transition. Mol. Cell **43**, 811–822

Received 13 August 2012/13 September 2012; accepted 19 September 2012
Published as BJ Immediate Publication 19 September 2012, doi:10.1042/BJ20121280

Biochem. J. (2013) **449**, 151–159 (Printed in Great Britain) doi:10.1042/BJ20121280

online data

SUPPLEMENTARY ONLINE DATA

Small-molecule inhibition of MLL activity by disruption of its interaction with WDR5

Guillermo SENISTERRA*[1], Hong WU*[1], Abdellah ALLALI-HASSANI*[1], Gregory A. WASNEY*[1], Dalia BARSYTE-LOVEJOY*, Ludmila DOMBROVSKI*, Aiping DONG*, Kong T. NGUYEN*, David SMIL*, Yuri BOLSHAN*, Taraneh HAJIAN*, Hao HE*, Alma SEITOVA*, Irene CHAU*, Fengling LI*, Gennadiy PODA†, Jean-François COUTURE‡, Peter J. BROWN*, Rima AL-AWAR†, Matthieu SCHAPIRA*§, Cheryl H. ARROWSMITH*‖[2] and Masoud VEDADI*[2]

*Structural Genomics Consortium, 101 College Street, Toronto, Ontario, Canada, M5G 1L7, †Medicinal Chemistry Platform, Ontario Institute for Cancer Research, MaRS Centre, South Tower, 101 College Street, Toronto, Ontario, Canada, M5G 0A3, ‡Ottawa Institute of Systems Biology, Department of Biochemistry, Microbiology and Immunology, University of Ottawa, 451 Smyth Road, Ottawa, Ontario, Canada, K1H 8M5, §Department of Pharmacology and Toxicology, University of Toronto, 1 King's College Circle, Toronto, Ontario, Canada, M5S 1A8, and ‖Ontario Cancer Institute, The Campbell Family Institute for Cancer Research and Department of Medical Biophysics, University of Toronto, 1 King's College Circle, Toronto, Ontario, Canada, M5S 1A8

Criteria for selecting compounds for high-throughput screening

A 16 000 diverse set of compounds were selected from the Ontario Institute for Cancer Research general screening library. Application of the filters described below was followed by a dissimilarity assessment based on the ECFP_4 substructural fingerprints. Clustering of the diversity set with FCFP_4 fingerprints revealed 3983 clusters and 4018 singletons, and the largest cluster size was set at 19 structures to ensure sufficient diversity and coverage of chemical space. Calculation of physical properties and derivation of the dissimilarity set were performed with Pipeline Pilot v.8.0.

High-throughput screening filters

A set of elaborated substructure (SS) and SMARTS filters were applied to eliminate reactive and undesirable compounds such as acetylenes, acid halides, aldehydes, α-halo nitriles, anthracenes, azides, benzthiozolium-like, catechols, dicarbonyls, epoxides, haloalkyls, haloethylenes, halopyri(mi)dines, heptane-like, hydrazines, acyclic imines, Michael acceptors, pentafluorophenyls, peroxides, phosphates, pyrimidinetriones, quinones, sulfates, thioaldehydes, thioalchohols, thiohalogens, thioureas, thioamides and thiozolium-like. We also limited our set to compounds with no more than one nitro or two nitrile groups.

Physical property filters

We applied filters based on calculated physical properties to eliminate undesirable compounds. These properties included the molecular mass (MW) of the parent structure (MW = 300–500 Da), PSA (polar surface area) ($6 \leqslant$ PSA $\leqslant 250$), calculated octan-1-ol/water partition coefficient, *A*log*P* [1] ($-3 \leqslant A\log P \leqslant 6.5$), number of hydrogen-bond donors ($0 \leqslant$ HBDon $\leqslant 10$), number of hydrogen-bond acceptors ($1 \leqslant$ HBAcc $\leqslant 15$), number of freely rotatable bonds (Nrot $\leqslant 16$), number of rings (Num_Rings $\geqslant 1$), number of aromatic rings (Num_AromaticRings $\leqslant 7$), number of atoms carrying negative formal charge at pH 7 (Num_NegativeAtoms $\leqslant 2$), number of atoms carrying positive formal charge at pH 7 (Num_PositiveAtoms $\leqslant 2$), number of metal atoms (Num_Metals <1), fluorine atom count (F_Count $\leqslant 7$), chlorine atom count (Cl_Count $\leqslant 4$), bromine atom count (Br_Count $\leqslant 1$), iodine atom count (I_Count $\leqslant 1$) and boron atom count (B_Count <1).

[1] These authors contributed equally to this work.

[2] Correspondence may be addressed to either of these authors (email mvedadi@uhnres.utoronto.ca or carrow@uhnres.utoronto.ca).

The structures of the WDR5-01025–WDR5 and WDR5-0103–WDR5 co-crystals have been deposited in the PDB under codes 3SMR and 3UR4 respectively.

Table S1 Data collection and refinement statistics (molecular replacement) for WDR5 crystal structure in complex with WDR5-0102 and WDR5-0103

Values in parentheses are for the highest resolution shell. R_{work} is defined as $\Sigma||F_{obs}| - |F_{calc}|| / \Sigma|F_{obs}|$, where F_{obs} and F_{calc} are observed and calculated structure factor amplitudes respectively. R_{free} is the R factor for the test set (5–10 % of the data).

	3SMR	3UR4
Data collection		
Beamline	Rigaku FR-E SuperBright	Rigaku FR-E SuperBright
Wavelength (Å)	1.54	1.54
Space group	*C*2	*C*2
Cell dimensions		
a, *b*, *c* (Å)	204.2, 93.5, 64.8	134.8, 47.0, 112.9
α, β, γ (°)	90.0, 107.2, 90.0	90.0, 117.9, 90.0
Resolution (Å)	50.00–1.82	50.00–1.80 (1.83–1.80)
R_{sym}	0.086 (0.807)	0.042 (0.165)
$I/(\sigma I)$	25.0 (2.1)	22.2 (2.7)
Completeness (%)	100.0 (100.0)	98.1 (79.3)
Redundancy	7.2 (6.4)	3.9 (2.9)
Refinement		
Resolution (Å)	50.00–1.82	50.00–1.80
Number of reflections	103 163	56 017
R_{work}/R_{free}	0.177/0.206	0.182/0.213
Number of atoms		
Protein	9361	4754
Ligands	104	56
Water	820	717
B -factors (Å^2)		
Protein	25.1	18.8
Ligands	23.4	16.4
Water	34.8	30.5
RMSDs (root mean square deviations)		
Bond lengths (Å)	0.008	0.007
Bond angles (°)	1.134	1.109
Ramachandran plot		
Favoured regions (%)	96.2	96.1
Disallowed regions (%)	0.02	0.02

Table 2 Kinetic parameters for MLL core complexes

Experiments were performed in duplicate.

	K_m (μM)		
Protein complex	*S*-adenosylmethionine	Peptide	k_{cat} (h^{-1})
MLL–WDR5–RbBP5	2 ± 0.1	2 ± 0.1	3.5 ± 0.1
MLL–WDR5–RbBP5–ASH2L	2.6 ± 0.1	1.1 ± 0.1	27 ± 0.3

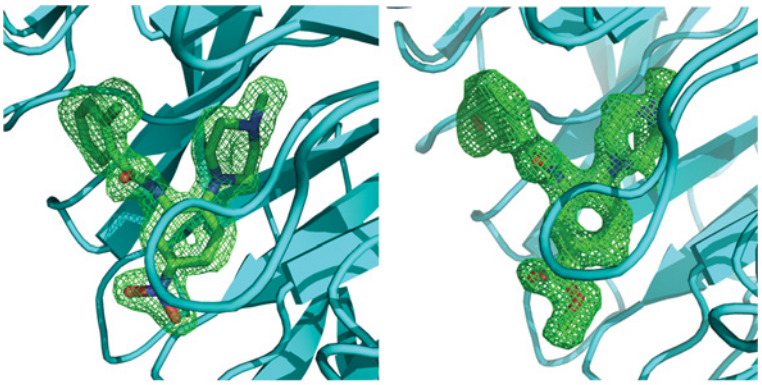

Figure S1 Omit maps of electron density for WDR5 antagonists

Total omit maps were calculated using SFCHECK [1] for both WDR5-0102 (PDB code 3SMR) and WDR5-0103 (PDB code 3UR4). Electron densities contoured at 1σ are shown.

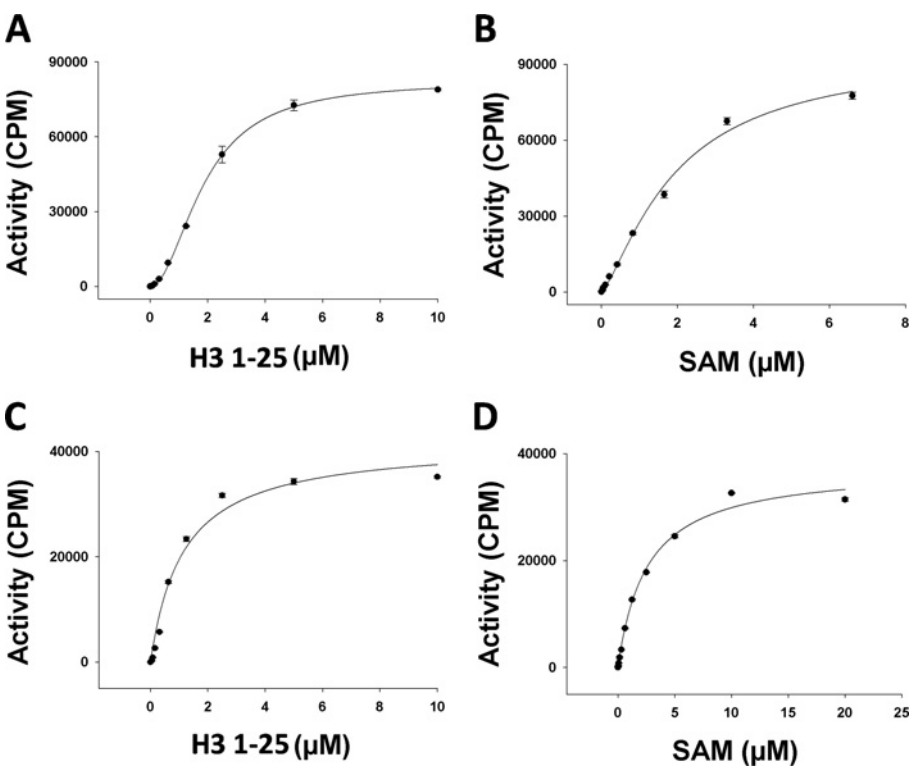

Figure S2 Kinetic parameters for MLL complexes

K_m values were determined for (**A**) peptide and (**B**) SAM (*S*-adenosylmethionine) for trimeric (MLL–WDR5–RbBP5) complex as well as (**C**) peptide and (**D**) SAM for tetrameric complex (MLL–WDR5–RbBP5–ASH2L). Kinetic values are presented in Supplementary Table S2. Experiments were performed in duplicate as described in the Materials and methods section of the main paper. Results are means $\pm$ S.D.

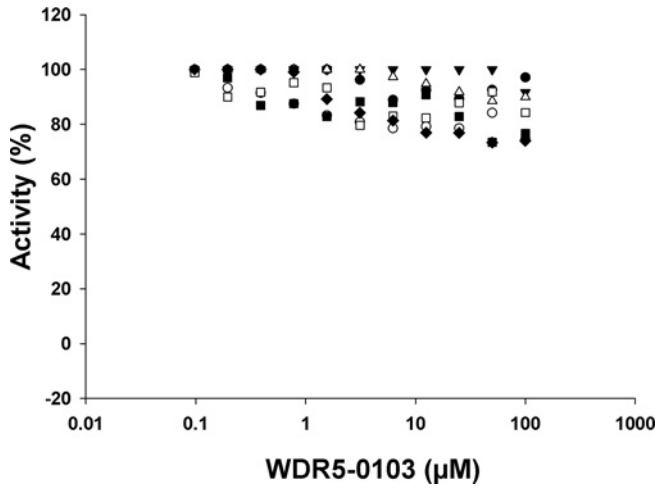

Figure S3 Selectivity of WDR5-0103

Inhibitory effect of WDR5-0103 on activity of (●) SETD7, (○) SETD8, (△) G9a, (■) EHMT1, (□) SUV39H2, (▼) PRMT3 and (◆) PRMT5_MEP50 complex were accessed at concentrations of compound ranging from 100 nM to 100 μM.

REFERENCE

1 Vaguine, A. A., Richelle, J. and Wodak, S. J. (1999) SFCHECK: a unified set of procedures for evaluating the quality of macromolecular structure-factor data and their agreement with the atomic model. Acta Crystallogr. Sect. D Biol. Crystallogr. **55**, 191–205

Received 13 August 2012/13 September 2012; accepted 19 September 2012
Published as BJ Immediate Publication 19 September 2012, doi:10.1042/BJ20121280